iScience

CellPress
OPEN ACCESS

Article

SARS-CoV-2 variant B.1.1.7 caused HLA-A2^{+} CD8^{+} T cell epitope mutations for impaired cellular immune response

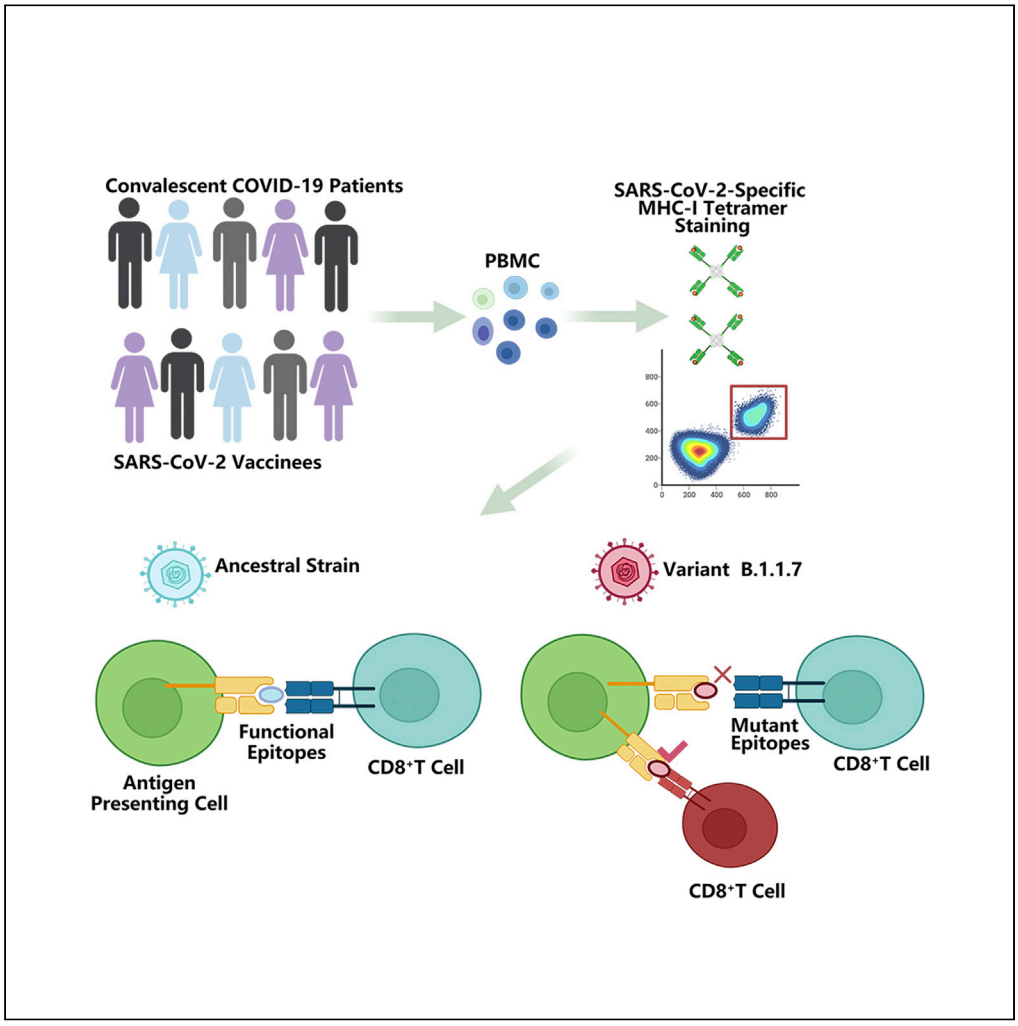

Chanchan Xiao, Lipeng Mao, Zhigang Wang, ..., Lianbo Xiao, Pengcheng Wang, Guobing Chen

13701888178@163.com (L.X.)
twangpc@jnu.edu.cn (P.W.)
guobingchen@jnu.edu.cn (G.C.)

Highlights

Impaired immune response in CD8^{+} T cells caused by mutant epitopes in B.1.1.7

Identification of the exact epitopes that caused impaired CD8^{+} T cell immune responses

Validation of vaccine still elicited over 60% of the immune protection against B.1.1.7

Xiao et al., iScience 25, 103934
March 18, 2022
https://doi.org/10.1016/j.isci.2022.103934

iScience

CellPress
OPEN ACCESS

Article

SARS-CoV-2 variant B.1.1.7 caused HLA-A2$^+$ CD8$^+$ T cell epitope mutations for impaired cellular immune response

Chanchan Xiao,[1,2,13] Lipeng Mao,[1,2,13] Zhigang Wang,[3,13] Lijuan Gao,[1,2,13] Guodong Zhu,[2,4] Jun Su,[3] Xiongfei Chen,[5] Jun Yuan,[5] Yutian Hu,[6] Zhinan Yin,[7] Jun Xie,[8,9] Weiqing Ji,[8,9] Haitao Niu,[10] Feng Gao,[11] Oscar Junhong Luo,[2,12] Lianbo Xiao,[8,9,*] Pengcheng Wang,[1,2,*] and Guobing Chen[1,2,3,14,*]

SUMMARY

Here, we evaluated the immune properties of the HLA-A2 restricted CD8$^+$ T cell epitopes containing mutations from B.1.1.7, and furthermore performed a comprehensive analysis of the SARS-CoV-2 specific CD8$^+$ T cell responses from COVID-19 convalescent patients and SARS-CoV-2 vaccinees recognizing the ancestral Wuhan strain compared to B.1.1.7. First, most of the predicted CD8$^+$ T cell epitopes showed proper binding with HLA-A2, whereas epitopes from B.1.1.7 had lower binding capability than those from the ancestral strain. In addition, these peptides could effectively induce the activation and cytotoxicity of CD8$^+$ T cells. Our results further showed that at least two site mutations in B.1.1.7 resulted in a decrease in CD8$^+$ T cell activation and a possible immune evasion, namely A1708D mutation in ORF1ab$_{1707\text{-}1716}$ and I2230T mutation in ORF1ab$_{2230\text{-}2238}$. Our current analysis provides information that contributes to the understanding of SARS-CoV-2-specific CD8$^+$ T cell responses elicited by infection of mutated strains or vaccination.

INTRODUCTION

The coronavirus disease 2019 (COVID-19) pandemic has been sweeping the world. Its etiological agent, severe acute respiratory syndrome coronavirus 2 (SARS-CoV-2) belongs to the *Betacoronovirus* genus of the Coronoviridae family, and this single-stranded positive-sensed RNA virus bears 11 protein-coding genes, including 4 for structural proteins: spike (S), envelope (E), membrane (M), nucleocapsid (N), and 7 for nonstructural proteins: open reading frame (ORF) 1ab, ORF 3a, ORF 6, ORF 7a, ORF 7b, ORF 8, and ORF 10 (Wu et al., 2020). It's believed that the viral clearance in SARS-CoV-2 infected individuals is mainly dependent on host immune system, especially adaptive immunity (Zhang et al., 2020). Specific antibodies have been observed in virus infected individuals and convalescent COVID-19 patients, with S and N being the major viral proteins to elicit antibody production (Wheatley et al., 2021). S protein bears the binding site to ACE 2 (ACE2) receptors on host cells and is crucial for viral infection. So the neutralizing antibodies against S protein are believed to play an important role for the virus clearance (Bertoglio et al., 2021). However, a couple of studies have shown that antibody titers decline fast in some convalescent patients (Seow et al., 2020; Ward et al., 2020). On the other hand, current studies have demonstrated that specific T cell responses emerge in most of the COVID-19 patients during the early stage of the infection (Ferreras et al., 2021). Although significant reduction in T cell counts was observed in severe COVID-19 patients, the revealed antigen specific T cell response indicated their important role in resolving SARS-CoV-2 infection (Grifoni et al., 2020; Le Bert et al., 2020; Weiskopf et al., 2020). Furthermore, SARS-CoV-2 specific CD8$^+$ T cells have been detected in convalescent COVID-19 patients (Braun et al., 2020; Grifoni et al., 2020; Gangaev et al., 2021) and SARS-CoV-2 vaccinees (Jackson et al., 2020). Recent studies have shown that specific CD8$^+$ epitopes to SARS-CoV-2 are mainly located in ORF1ab, N protein, S protein, ORF 3, M protein, and ORF 8 (Ferretti et al., 2020; Grifoni et al., 2020), and the identification of these epitopes will provide the basis for next-generation vaccine development and better understanding of CD8$^+$ T cell immunity.

With the ongoing spreading of the virus all over the world, the genetic evolution in SARS-CoV-2 continues to provide the opportunities for the virus to obtain mutations which might contribute to the changes in viral

Continued

[1]Department of Microbiology and Immunology, Institute of Geriatric Immunology, School of Medicine, Jinan University, Guangzhou 510000, China

[2]Guangdong-Hong Kong-Macau Great Bay Area Geroscience Joint Laboratory, Guangzhou 510000, China

[3]Affiliated Huaqiao Hospital, Jinan University, Guangzhou 510000, China

[4]Department of Geriatrics, Guangzhou First People's Hospital, School of Medicine, South China University of Technology, Guangzhou 510000, China

[5]Guangzhou Center for Disease Control and Prevention, Guangzhou 510000, China

[6]Meng Yi Center Limited, Macau 999078, China

[7]Biomedical Translational Research Institute, Jinan University, Guangzhou 510000, China

[8]ShangHai GuangHua Hospital of Integrated Traditional Chinese and Western Medicine, Shanghai 200052, China

[9]Arthritis Institute of Integrated Traditional Chinese and Western Medicine, Shanghai Academy of Traditional Chinese Medicine, Shanghai University of Chinese Traditional Medicine, Shanghai 200052, China

[10]School of Medicine & Institute of Laboratory Animal Sciences, Jinan University, Guangzhou 510000, China

[11]School of Medicine, Jinan University, Guangzhou 510000, China

transmissibility, infectivity, pathogenesis, and even immune evasion (Neches et al., 2021; Rashid et al., 2021). The D614G spike variant emerged in March 2020 was the earliest evidence of adaptive evolution of the virus in humans, which resulted in increased infectivity of the virus (Yurkovetskiy et al., 2020). Recently, a newer variant termed B.1.1.7 (also called VUI202012/01) was spreading rapidly in the United Kingdom (UK) and raised great concerns (Davies et al., 2021; Kirby, 2021). This variant contains 17 non-synonymous mutations in ORF1ab, S protein, ORF8 and N proteins, some of which are of particular concerns, such as the D614G mutation and eight additional mutations in S protein: ΔH69-70, ΔY144, N501Y, A570D, P681H, T716I, S982A, and D1118H (Davies et al., 2021). For example, N501Y is located in the receptor binding motif (RBM) and P681H is proximal to the furin cleavage site (Peacock et al., 2020; Starr et al., 2020). ΔH69-70 in S protein has evolved in other lineages of SARS-CoV-2, which enhances viral infectivity *in vitro* and is linked to immune escape in immunocompromised patients (Kemp et al., 2020a, 2020b). There is strong evidence that variant B.1.1.7 is spreading substantially faster than preexisting SARS-CoV-2 variants (Davies et al., 2021; Kemp et al., 2020b; Volz et al., 2021). The model analysis suggests that this difference could be explained by an overall higher infectiousness of variant B.1.1.7. However, it is not clear that this is because of the shorter generation time or immune escape (Davies et al., 2021). Mutations in immune dominant epitopes might potentially alter their immunogenicity, and subsequently the immune responses of the host.

Our previous work has shown that the mutations in given $CD8^+$ T cell epitopes resulted in antigen presentation deficiency and impaired antigen specific T cell function, indicating an immune evasion induced by viral evolution (Qiu et al., 2020; Xiao et al., 2021). In this work, we predicted the potential $CD8^+$ T cell epitopes within the areas where these mutations are located, and compared the immune properties of the ancestral and mutant peptides, including MHC I binding and activation of $CD8^+$ T cells. Furthermore, we detected the epitope specific $CD8^+$ T cells in convalescent COVID-19 patients and SARS-CoV-2 vaccinees by using corresponding tetramers. The results showed that at least two site mutations in the variant B.1.1.7 resulted in a decrease in $CD8^+$ T cell activation and a possible immune evasion, namely A1708D mutation in $ORF1ab_{1707\text{-}1716}$ and I2230T mutation in $ORF1ab_{2230\text{-}2238}$. Our current analysis provides useful information that helps for better understanding of the SARS-CoV-2-specific $CD8^+$ T cell responses elicited by infection of mutated strains or vaccination.

RESULTS

Identification of potential T cell epitopes containing mutations in B.1.1.7

During late 2020, the WHO (WHO) announced the emergence of a novel coronavirus variant B.1.1.7 in the UK. We immediately carried out HLA-A2-restricted T cell epitope screening and identification of all the possible peptides containing the mutations in B.1.1.7 by using the high-throughput screening platform and artificial antigen presentation system for epitopes (Figures 1A and 1B; Table S1). To validate these predicted epitopes, we first checked whether they could be presented by HLA-A2 on the antigen-presenting cells (APC). T2A2 is an APC with TAP deficiency and HLA-A2 expression on cell surface. The peptide-MHC complex would be more stabilized if the epitopes bind with HLA-A2 suitably. Compared with the negative control peptide GLQ (GLQRLGYVL) from Zika virus, most of the predicted SARS-CoV-2 epitopes showed reasonable HLA-A2 binding. However, the HLA-A2 binding of most of the epitopes from the variant B.1.1.7 was reduced (Figures 1C and 1D). We further checked the direct binding of these epitopes to the purified HLA-A2 protein. According to the UV exchanged peptide-MHC assay, all the peptides, except for N S235F, exhibited strong binding to HLA-A2 (Figure 1E). The results indicated that the majority of the predicted epitopes could form peptide-MHC complex (pMHC), and corresponding tetramers could be constructed next.

Activation and cytotoxicity of T cells stimulated with T cell epitopes containing mutations of B.1.1.7

To further analyze whether the epitope-bound T2A2 cells could activate T cells, we tested the expression level of T cell activation marker CD69 and the proportion of peptide-specific $CD8^+$ T cells after stimulation with peptide-bound T2A2 cells. As shown in Figures 2A and 2B, T2A2 cells bearing peptides of ancestral and B.1.1.7 induced significant increase in CD69 expression, respectively (Figures 2A and 2B). Further, our results showed that two mutations, namely A1708D in peptide $ORF1ab_{1707\text{-}1716}$ and I2230T in peptide $ORF1ab_{2230\text{-}2238}$ induced dramatically less proportion of specific $CD8^+$ T cells than ancestral in the same subject. Intriguingly, the I2230T mutation in peptide $ORF1ab_{2225\text{-}2234}$ did not result in similar decrease in T cell activation (Figures 2C–2E and S1A–S1C), and representative data and a gating strategy are shown in (Figure S2A). Next, we performed cross-detection of ancestral peptide specific $CD8^+$ T cells with

[12]Department of Systems Biomedical Sciences, School of Medicine, Jinan University, Guangzhou 510000, China

[13]These authors contributed equally

[14]Lead contact

*Correspondence: 13701888178@163.com (L.X.), twangpc@jnu.edu.cn (P.W.), guobingchen@jnu.edu.cn (G.C.)

https://doi.org/10.1016/j.isci.2022.103934

A

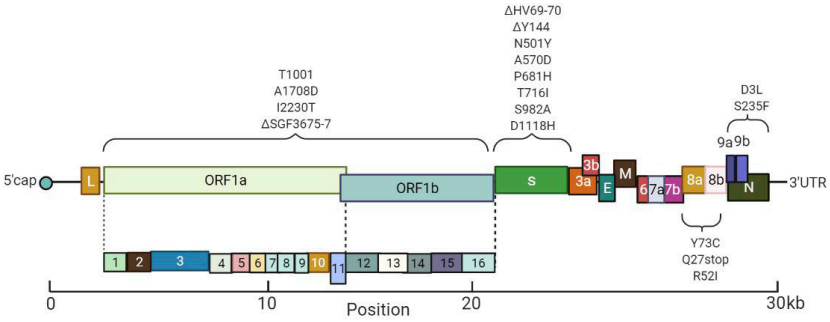

B

Protein	Number	Ancestral/mutant	Start position	End position	Length	Sequence	Antigenic value[a]
ORF1ab	01	Ancestral	1000	1008	9	TTIQTIVEV	0.1250
	02	T1001I	1000	1008	9	TIIQTIVEV	-0.1557
	03	Ancestral	1707	1716	10	AANFCALILA	0.4442
	04	A1708D	1707	1716	10	ADNFCALILA	0.4489
	05	Ancestral	2225	2234	10	KLINIIIWFL	0.1004
	06	I2230T-1	2225	2234	10	KLINITIWFL	0.5790
	07	Ancestral	2230	2238	9	IIWFLLLSV	0.7365
	08	I2230T-2	2230	2238	9	TIWFLLLSV	0.6152
	09	Ancestral	3673	3683	11	SLSGFKLKDCV	0.5452
	10	ORF1abΔSGF3675-7	3673	3683	8	SLKLKDCV	0.7220
	11	Ancestral	3672	3683	12	TSLSGFKLKDCV	0.4410
	12	ORF1abΔSGF3675-7	3672	3683	9	TSLKLKDCV	0.7545
Spike	13	Ancestral	62	70	9	VTWFHAIHV	0.5426
	14	S ΔHV69-70	62	70	9	VTWFHAISG	0.2071
	15	S ΔY144-1	135	145	10	FCNDPFLGVY	0.2713
	16	Ancestral	136	145	10	CNDPFLGVYY	0.4496
	17	S ΔY144-2	136	145	9	CNDPFLGVY	0.4295
	18	Ancestral	495	503	9	YGFQPTNGV	1.0509
	19	N501Y	495	503	9	YGFQPTYGV	1.0317
	20	Ancestral	567	576	10	RDIADTTDAV	0.6138
	21	A570D	567	576	10	RDIDDTTDAV	0.7119
	22	Ancestral	673	684	12	SYQTQTNSPRRA	0.0145
	23	P681H	673	684	12	SYQTQTNSHRRA	0.3119
	24	Ancestral	713	722	10	AIPTNFTISV	0.8945
	25	T716I	713	722	10	AIPINFTISV	1.5957
	26	Ancestral	976	984	9	VLNDILSRL	-0.8524
	27	S982A	976	984	9	VLNDILARL	-0.6998
	28	Ancestral	1114	1122	9	IITTDNTFV	0.4733
	29	D1118H	1114	1122	9	IITTHNTFV	0.4551
ORF8	30	Ancestral	73	81	9	YIDIGNYTV	1.3128
	31	Y73C	73	81	9	CIDIGNYTV	2.0234
	32	Ancestral	18	27	10	QECSLQSCTQ	-0.5395
	33	Q27stop	18	27	9	QECSLQSCT	-0.7637
	34	Ancestral	50	58	9	GARKSAPLI	0.8210
	35	R52I	50	58	9	GAIKSAPLI	0.7366
N	36	Ancestral	1	9	9	MSDNGPQNQ	0.0243
	37	D3L	1	9	9	MSLNGPQNQ	-0.3554
	38	Ancestral	228	236	9	NQLESKMSG	0.4574
	39	S235F	228	236	9	NQLESKMFG	0.2619

C

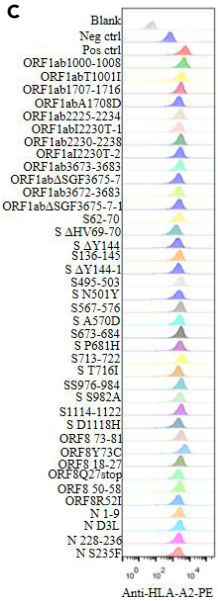

D

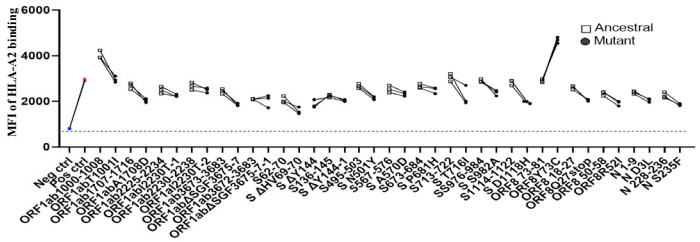

E

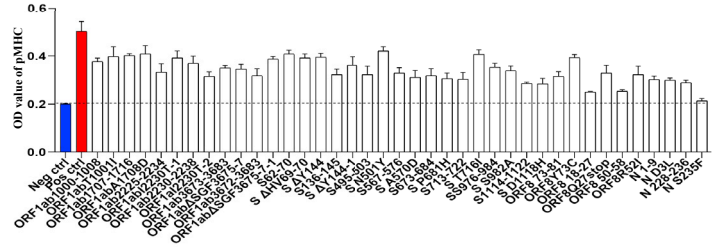

Figure 1. Identification of HLA-A2 restricted T cell epitopes on SARS-CoV-2 variant B.1.1.7

(A) The schematic of mutation sites of the SARS-CoV-2 variant B.1.1.7.

(B) List of the predicted epitopes for following experiments. The mutated amino acids were highlighted as red in varian B.1.1.7. [a]The antigenic value threshold was >0.4 (http://www.ddg-pharmfac.net/vaxijen/VaxiJen/VaxiJen.html).

(C and D) Comparison of ancestral and mutant epitope binding affinity to HLA-A2 in T2A2 cells. Ancestral and mutated epitopes were synthesized and 20 μM of each peptide was incubated with T2A2 cells. The binding of the peptide on T2A2 was measured with anti-HLA-A2 staining with flow cytometry. Binding capacity was presented as mean fluorescence intensity (MFI) of HLA-A2 staining. (C) was the representative plot of (D). Each symbol represents an independent experiment. Ancestral: Wuhan strain epitope; Mutant: varian B.1.1.7 epitope.

(E) Evaluation of epitope binding to HLA-A2 with ELISA assay. Peptide exchanged assay was performed with coated UV-sensitive peptide/MHC (pMHC) complex and given peptides. The binding capability was measured with pMHC ELISA assay. Threshold for pMHC formation positivity was set as above the average OD value of the negative-control cohort. Data shown are mean +/− SE of the mean (SEM). Consistent mean ± SEM are used throughout the paper. Blank: no peptides; Neg ctrl: negative control, Zika virus peptide GLQRLGYVL; Pos ctrl: positive control, influenza An M1 peptide GILGFVFTL.

tetramers containing mutant peptides, and vice versa. The results showed that $CD8^+$ T cells stimulated with the mutant peptides could not be recognized by tetramers containing the ancestral peptides (Figures 2F and 2G), nor could $CD8^+$ T cells stimulated with the ancestral peptides be recognized by tetramers containing the mutant peptides (Figures 2H and 2I). Furthermore, both ancestral and mutant peptide-bound T2A2 cells stimulated T cell-mediated T2A2 killing. However, the mutant peptide group had a higher proportion of survival target cells compared to the ancestral group, suggesting a decreased cytotoxicity from mutant peptide specific $CD8^+$ T cells (Figures 3A and 3B), and representative data and a gating strategy are shown in (Figure S2C). In addition, the proportion of CFSE-Annexin V^+ T2A2 was less for the mutant peptide group than that for the ancestral peptide group, indicating less T cell-mediated target cell apoptosis (Figures 3C and 3D). Finally, the $CD8^+$ IFN-γ (Figures 3E and 3F) and Granzyme B (Figures 3G and 3H) levels in mutant peptide group were significantly lower than those in ancestral peptide group, and representative data and a gating strategy are shown in (Figure S2B). All the above results suggested that, compared to the ancestral, T cell mediated immune responses induced by B.1.1.7 mutant peptides were impaired.

SARS-CoV-2-specific $CD8^+$ T cell profiling in convalescent COVID-19 patients and SARS-CoV-2 vaccinees

We recruited a cohort of 25 convalescent COVID-19 patients and 60 SARS-CoV-2 vaccinees, including 4 and 17 who were HLA-A2 positive, respectively. The demographic and clinical information of the patients with $tetramer^+$ cells were presented in Table S2. We examined the *ex vivo* phenotypes of SARS-CoV-2 $tetramer^+$ $CD8^+$ T cells in PBMCs of the patients by assessing the expression levels of the chemokine receptor CCR7 and CD45RA. It's observed that the tetramers prepared with the above identified epitopes could recognize the specific memory T cells in convalescent patients (Figures 4A and 4B). MHC class I $tetramer^+$ cells predominantly exhibited an effector memory ($CCR7^-CD45RA^-$) phenotype (Figures 4C and 4D). Meanwhile, in the same individual, the proportion of T cells recognized by the B.1.1.7 mutant epitope tetramers was lower than that by the ancestral epitope tetramers (Figure 4B). We then examined the differentiation phenotype of SARS-CoV-2 specific $CD8^+$ T cells in vaccinees, with the information of the subjects presented in Table S3. It's observed that the tetramers prepared with the above identified epitopes could recognize the specific memory T cells (Figures 5A–5C), and the majority of $tetramer^+$ cells were memory T ($CCR7^+CD45RA^-$) phenotype (Figures 5D and 5E). Similarly, the proportion of T cells recognized by the B.1.1.7 mutant epitope tetramers was lower than that by the ancestral epitope tetramers in the same individual (Figure 5B). All above data indicated that these emerged mutations might have caused a deficiency in the antigen presentation of the dominant epitopes, which was required to rebuild a new $CD8^+$ T cell immune response in COVID-19 patients and vaccinees.

Computational molecular docking simulation of ancestral and B.1.1.7 epitopes with HLA-A2

To further explore the binding pattern between peptides and HLA-A2, molecular docking model was established with Galaxypepdock, and pairwise comparison of pMHC structure was performed between $ORF1ab_{1707\text{-}1716}$ and ORF1ab A1708D, $ORF1ab_{2225\text{-}2234}$ and ORF1ab I2230T-1, and $ORF1ab_{2230\text{-}2238}$ and ORF1ab I2230T-2, respectively. It's observed that these mutations slightly decreased the interaction similarity of mutant peptides to HLA-A2 (Figure 6A). Interestingly, subtle structural alterations of peptides presented by HLA-A2 were observed before and after mutation. Molecular docking comparison between $ORF1ab_{1707\text{-}1716}$ (Figure 6B, blue) and ORF1ab A1708D (Figure 6B, red) showed A1708D mutation caused deflection of the benzene ring of the subsequent asparagine (N) (Figure 6C, angle from 145.4° to 101.8°). Modeling of $ORF1ab_{2225\text{-}2234}$ (Figure 6D, blue) and

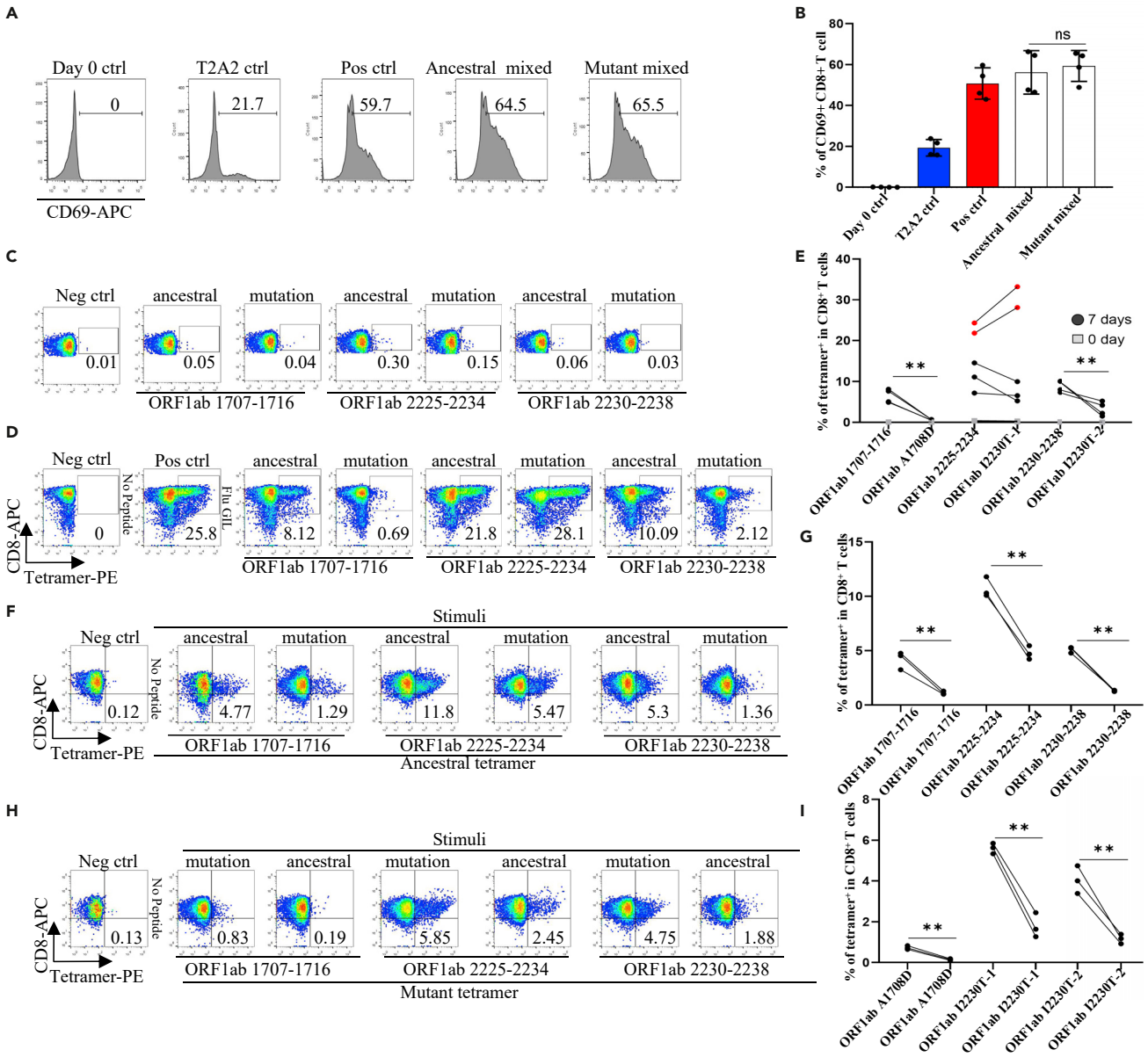

Figure 2. Activation of CD8$^+$ T cell by peptides on SARS-CoV-2 variant B.1.1.7 protein

Mitomycin pretreated T2A2 cells were loaded with mixed peptides from ancestral or mutant, and incubated with CD8$^+$ T cells from health donors at 1:1 ratio, respectively. Activation, cytotoxicity, and generation of epitope specific CD8$^+$ T cells were evaluated.

(A and B) The expression level of CD8$^+$ T cell activation marker CD69. CD8$^+$ T cells from healthy donors were cocultivated with T2A2 cells loaded with various peptides, including Neg ctrl, T2A2 ctrl, and T2A2 cells with mixed candidate peptides. CD69 expression was detected by using flow cytometry 16 h after cocultivation. (A) was the representative plot of (B) n = 4 per group. Day 0 ctrl: staining before stimulation; T2A2 ctrl: T2A2 without peptide loading; Pos ctrl: T2A2 loaded with influenza An M1 peptide GILGFVFTL; ns: not statistically significant ($p > 0.05$).

(C–E) Epitope specific CD8$^+$ T cell measurement before (C) and after (D) 7 days stimulation. Representative FACS plots of specific CD8$^+$ T cells recognized by tetramers containing candidate peptides. CD8$^+$ T cells from healthy donors were cocultivated with T2A2 cells loaded with various peptides for activation. The cells were stained with corresponding ancestral or mutated tetramer, and compared before (day 0) and after (day 7) stimulation. (E) Four and five repeats were performed for decreased and unchanged comparison, respectively. Please also see Figures S1A–S1C and S2A. **$p < 0.01$. Neg ctrl: Zika virus peptide GLQRLGYVL; Pos ctrl: T2A2 loaded with influenza An M1 peptide GILGFVFTL. F-I: Cross-detection of epitope specific CD8$^+$ T cells with tetramers based on ancestral and corresponding mutant peptides.

(F and G) ancestral or mutant epitopes stimulated CD8$^+$ T cells were stained with ancestral peptide-based tetramer.

(H and I) mutant or ancestral epitopes stimulated CD8$^+$ T cells were stained with mutant peptide-based tetramer. n = 3 per group. Symbols in G and I represented an individual person. The p values were calculated by paired-samples T test. **$p < 0.01$. Neg ctrl: Zika virus peptide GLQRLGYVL; Pos ctrl: T2A2 loaded with influenza An M1 peptide GILGFVFTL.

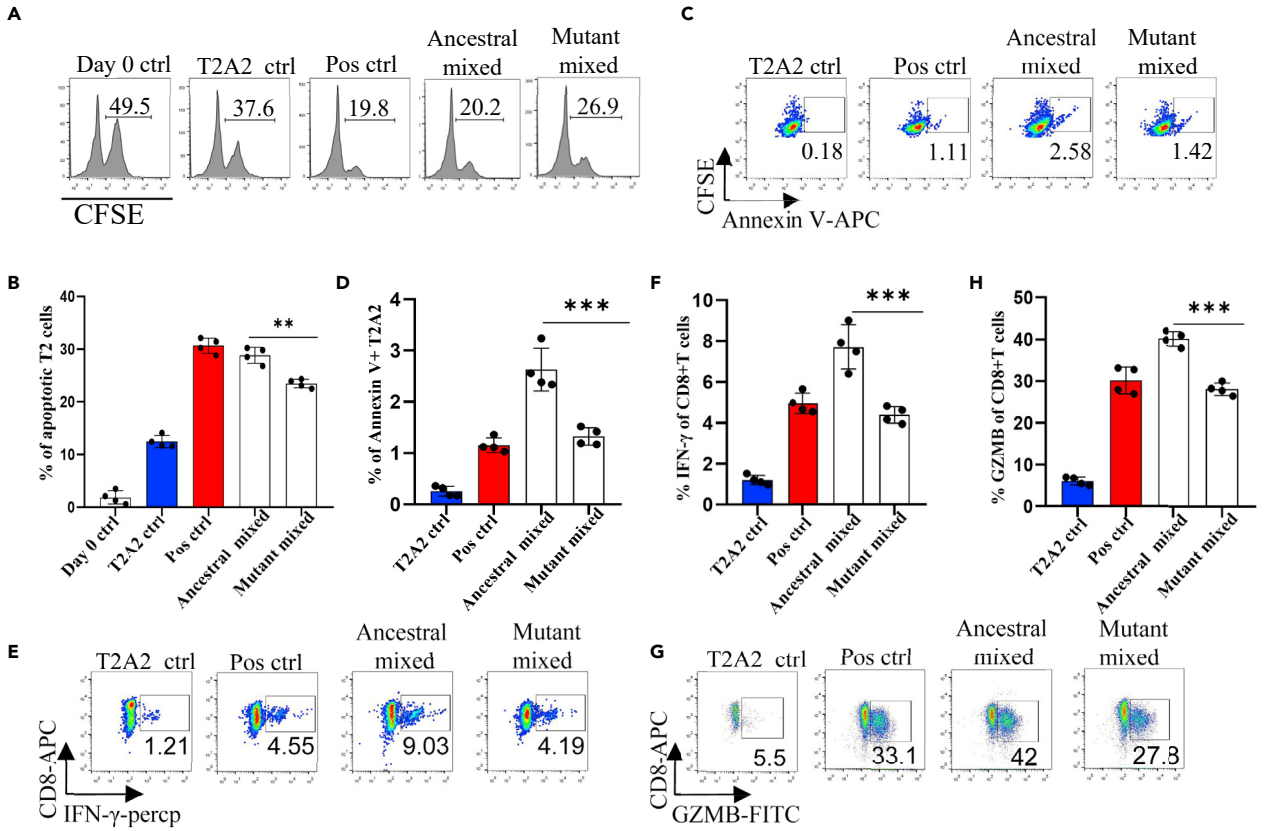

Figure 3. Evaluation of impaired immune protection caused by epitope mutation in SARS-CoV-2 variant B.1.1.7

(A–D) Epitope specific CD8$^+$ T cell mediated cytotoxicity was evaluated after 7 days culture (A and B). The remained CFSE labeled T2A2 cells were calculated as survived target cells. The percentage of apoptotic cells in T2A2 cells presenting distinct SARS-CoV-2 antigens after 7 days culturing with CD8$^+$ T cells, calculated by 50% of T2A2 cells minus the percentage of surviving cells. (A) was the representative plot of (B). Apoptosis of T2A2 cells at day 7 after culture. The proportion of CFSE$^+$ AnnexinV$^+$ cells was calculated as an indicator for epitope stimulated T cell mediated T2A2 apoptosis (C and D). (C) was the representative plot of (D) n = 4 per group. Please also see Figure S2C.

(E and F) The expression of IFN-γ after epitope stimulation for 7 days. IFN-γ was measured with intracellular stained flow cytometry. (E) was the representative plot of (F) n = 4 per group. Please also see Figure S2B.

(G and H) The expression of Granzyme B after epitope stimulation for 7 days. Granzyme B was measured with intracellular stained flow cytometry. (G) was the representative plot of (H) n = 4 per group. Please also see Figure S2B. Day 0 ctrl: staining before stimulation; T2A2 ctrl: T2A2 without peptide loading; Pos ctrl: T2A2 loaded with influenza An M1 peptide GILGFVFTL. The p values were calculated by paired-samples T test, **p < 0.01, ***p < 0.001.

ORF1ab I2230T-1 (Figure 6D, red) showed that the I2230T mutation herein might affect the later tryptophan (W), making the two benzene rings more convex (Figure 6E, angle from 66.7° to 92.2°). Modeling of ORF1ab$_{2230\text{-}2238}$ (Figure 6F, blue) and ORF1ab I2230T-2 (Figure 6F, red) showed that tryptophan (W) was more convex, and its benzene ring tended to expand (Figure 6G, angle from 0 to 66.6°). These structural changes might provide the possible molecular basis for the altered antigen presentation and CD8$^+$ T cell activation, whereas further protein crystallographic analysis is needed for confirmation.

DISCUSSION

The soaring rise of SARS-CoV-2 infection in the last months of 2020 has led to the evolution of several variants with related mutations or characteristics (Lauring and Hodcroft, 2021). One such variant, designated B.1.1.7, was identified in the UK during late 2020 and continued to dominate the circulation in the region. Recent studies have reported longer persistence and higher viral loads in samples from B.1.1.7 infected individuals, indicating its association with the higher infectivity and transmissibility (Calistri et al., 2021; Parker et al., 2021). It's also reported that B.1.1.7 might even lead to more severe illness (Challen et al., 2021). Our study aimed to fill a key knowledge gap addressing the potential of SARS-CoV-2 variants to evade recognition by human immune responses. Based on the mutation sites in B.1.1.7, we performed computational prediction of HLA-A2-restricted CD8$^+$ T cell epitopes, and obtained 19 potential epitopes for ancestral Wuhan strain and 20 for variant B.1.1.7, respectively. To validate

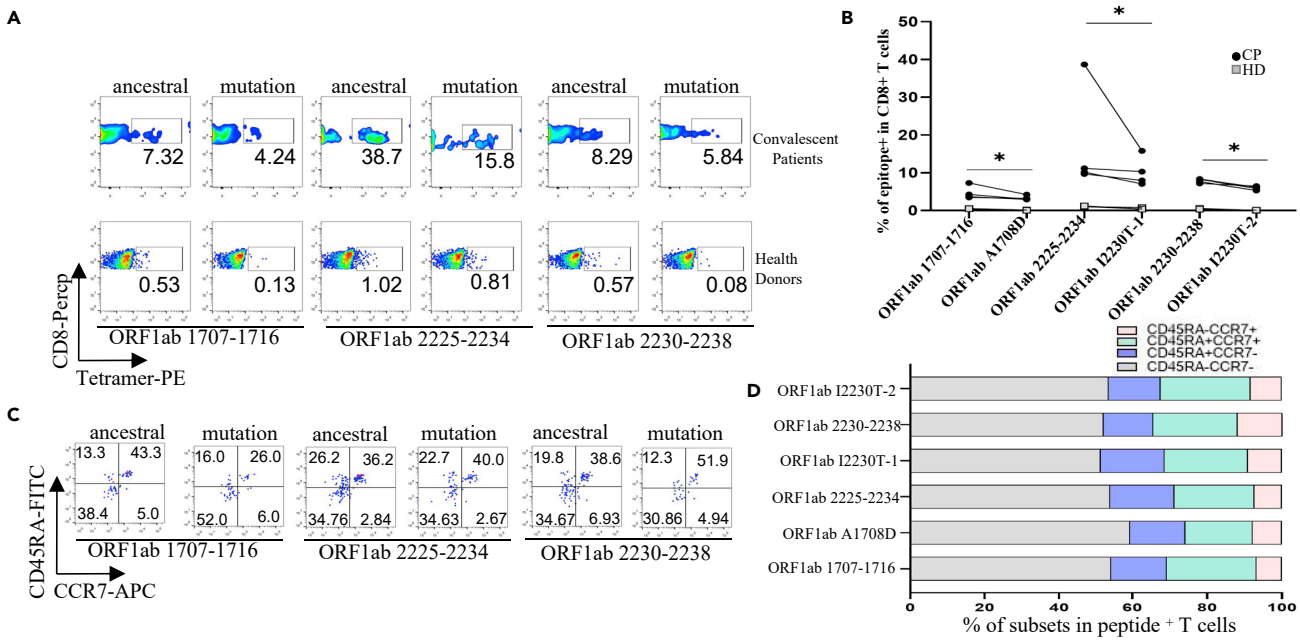

Figure 4. Profiling of epitope specific CD8$^+$ T cells in convalescent COVID-19 patients

(A–D) Ancestral and mutant peptide specific CD8$^+$ T cells (A and B) and functional subtypes (C and D) in HLA-A2$^+$ convalescent COVID-19 patients and healthy donors. HLA-A2 positive PBMCs samples were stained with PE labeled tetramer, PerCP labeled human CD8$^+$ antibody, APC labeled human CCR7 antibody, and FITC labeled human CD45RA antibody, and were acquired with flow cytometry. Ancestral and mutant epitope specific CD8$^+$ T cells in the same individual were compared in (B) n = 4 per group. The p values were calculated by paired-samples T test. *p < 0.05.

the binding of these predicted epitopes, we then checked whether they could be presented on T2A2 cells, where the peptide-MHC complex would be more stabilized if the epitopes bind with HLA-A2 suitably. Our results showed that most of the peptides had reasonable binding with HLA-A2, whereas the binding capability of most mutant peptides was lower than that of the ancestral. Recently, Tarke et al. reported an identification of 523 CD8$^+$ T cell epitopes associated with unique HLA restrictions (Tarke et al., 2021a), and 508 (97.1%) of them were totally conserved within the B.1.1.7 mutant (Tarke et al., 2021b), which might be a reason why they did not see significant difference in the T cell reactivity to the ancestral and mutant peptides. By using computational prediction, they reported 73.3% of the mutations were not associated with decrease in binding capacity (Tarke et al., 2021b). The difference of the results may be because of the different verification methods for the binding ability of SARS-CoV-2 T cell epitopes.

Up to date, SARS-CoV-2 mutations of most concern existed in the viral spike protein, including notable mutations in the receptor binding domain (RBD), N-terminal domain (NTD), and furin cleavage site region. Several of these mutations directly affect ACE2 receptor binding affinity, which may subsequently alter the infectivity, viral load, or transmissibility (Greaney et al., 2021; Zahradnik et al., 2021). Accordingly, it is crucial to address to what extent the mutations from the variants would impact the immunity induced by either SARS-CoV-2 variant infection or vaccination. Currently, most of the studies about immune responses against B.1.1.7 are focusing on alteration of humoral immunity. With neutralization assay to pseudovirus bearing B.1.1.7 spike protein, multiple specific mAbs showed resistance to B.1.1.7 pseudovirus (Collier et al., 2021; Muik et al., 2021). Furthermore, slightly but significantly decreased sensitivity was observed to the sera from SARS-CoV-2 vaccinees and convalescent patients (Muik et al., 2021; Wang et al., 2021). SARS-CoV-2 vaccine clinical trial data demonstrated that specific CD8$^+$ response was elicited as well as antibody production (Sahin et al., 2020), and the rapid emergence of the protection at the time when antibodies were still low further supported the important role of cellular immunity (Polack et al., 2020).

So far, the only report assessing the cellular immunity against B.1.1.7 is from Tarke et al., in which they evaluated the CD8$^+$ T cell reactivity in convalescent patients by using proteome-wide overlapping peptide megapools, and reported similar responses between ancestral and B.1.1.7 (Tarke et al., 2021b). In our study, altered CD8$^+$ T cell response was observed for particular CD8$^+$ epitopes. Our results first did show that mixed epitope-loaded

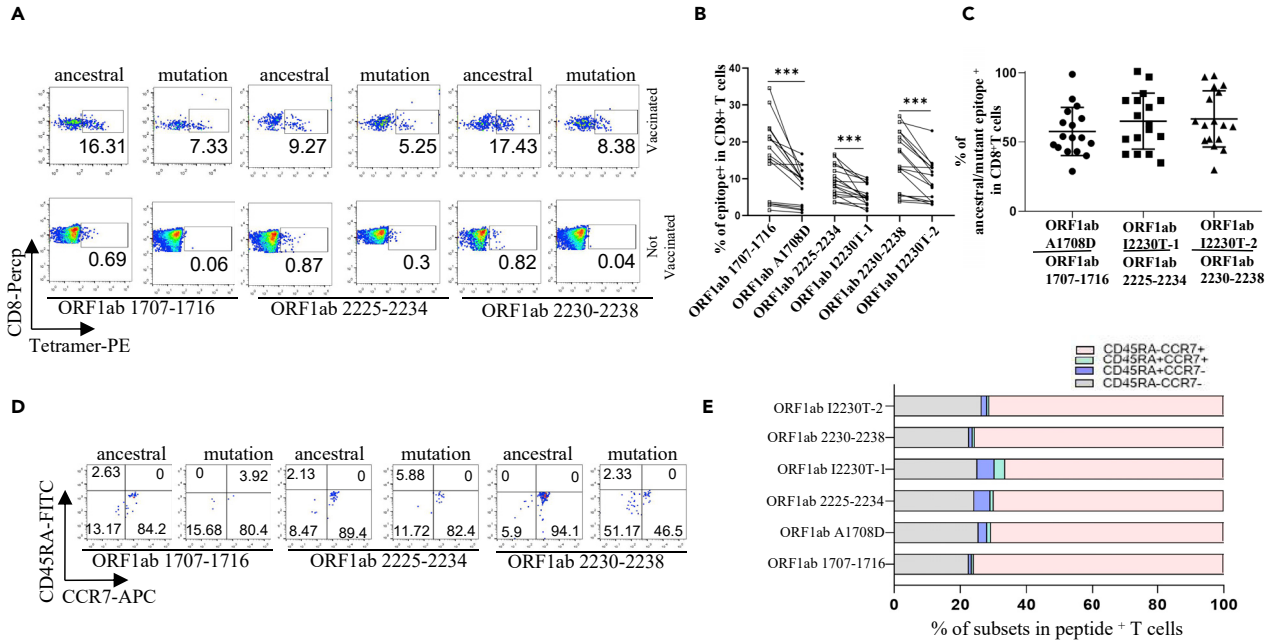

Figure 5. Profiling of epitope specific CD8$^+$ T cells in SARS-CoV-2 vaccinees

(A–E) PBMCs were collected from HLA-A2$^+$ vaccinees 1-3 months after SARS-CoV-2 vaccination. Ancestral and mutant peptide specific CD8$^+$ T cells (A and B) and functional subtypes (D and E). HLA-A2 positive PBMCs samples were stained with PE labeled tetramer, PerCP labeled human CD8$^+$ antibody, APC labeled human CCR7 antibody, and FITC labeled human CD45RA antibody, and were acquired with flow cytometry. The ancestral and mutant epitope specific CD8$^+$ T cells in the same individual were compared in (B), with ration calculation in (C). n = 17 per group. The p values were calculated by paired-samples T test, ***p < 0.001.

antigen presentation cells could activate T cells from healthy donors. Notably, the proportion of CD8$^+$ T cells specific to certain mutant peptides was less than that to ancestral in the same host. In addition, the ancestral epitope specific CD8$^+$ T cells could not be recognized by tetramers prepared with mutant epitopes, and vice versa. All these results showed that the T cell mediated immune responses induced by variant B.1.1.7 were decreased. Our previous work has also shown that the L > F mutations in spike protein epitope FVF*L*VLVPLV resulted in antigen presentation deficiency and reduced specific T cell function, indicating an immune evasion induced by viral evolution (Qiu et al., 2020). However, the impaired immune responses were further confirmed with the epitope specific CD8$^+$ T cells measurement from convalescent COVID-19 patients and SARS-CoV-2 vaccinees. In 25 convalescent COVID-19 patients, of whom only four were HLA-A2 positive, and in a larger sample set of confirmed infections should be studied to confirm these findings. Both results demonstrated that the proportion of T cells recognized by the mutant epitopes of B.1.1.7 was lower than that of the ancestral epitopes in the same individual. In summary, our results indicated that variant B.1.1.7 caused CD8$^+$ T cell epitopes mutation, which impaired the CD8$^+$ T cell immune response. However, our data showed that the vaccine we used still elicited over 60% of the immune protection against B.1.1.7 based on the cellular immune responses. Our data strongly indicated that mutant epitopes in SARS-CoV-2 variant B.1.1.7 caused deficiency in antigen presentation and CD8$^+$ T cell immune responses. It's required to rebuild a new CD8$^+$ T cell immune response for variant B.1.1.7.

Limitations of the study

Our current analysis provides information that contributes to the understanding of SARS-CoV-2-specific CD8$^+$ T cell responses elicited by infection of mutated strains or vaccination. However, it is unclear how much of an impact those escapes have on overall immunity during viral infection. In 25 convalescent COVID-19 patients, of whom only four were HLA-A2 positive, and in a larger sample set of confirmed infections should be studied to confirm these findings. Furthermore, our study focused on HLA-A*02 restricted epitopes currently, and other HLA class I allotype restricted CD8$^+$ T cells specific epitopes should be included for a broader understanding of SARS-CoV-2 induced immune responses, which shall be addressed in further studies.

STAR★METHODS

Detailed methods are provided in the online version of this paper and include the following:

A

Name	Sequence	Protein template	Peptide template	Protein structure similarity (TM-score)	Interaction similarity score	Estimated accuracy
ORF1ab 1707-1716	**AANFCALILA**	2X4S_A	2X4S_C	0.984	263.0	1.000
ORF1ab A1708D	**ADNFCALILA**	2X4S_A	2X4S_C	0.984	251.0	1.000
ORF1ab 2225-2234	**KLINIIIWFL**	3V5K_A	3V5K_C	0.985	250.0	1.000
ORF1ab I2230T-1	**KLINITIWFL**	3V5K_A	3V5K_C	0.985	250.0	1.000
ORF1ab 2230-2238	**IIWFLLLSV**	3H7B_A	3H7B_C	0.989	249.0	1.000
ORF1ab I2230T-2	**TIWFLLLSV**	3H7B_A	3H7B_C	0.989	249.0	1.000

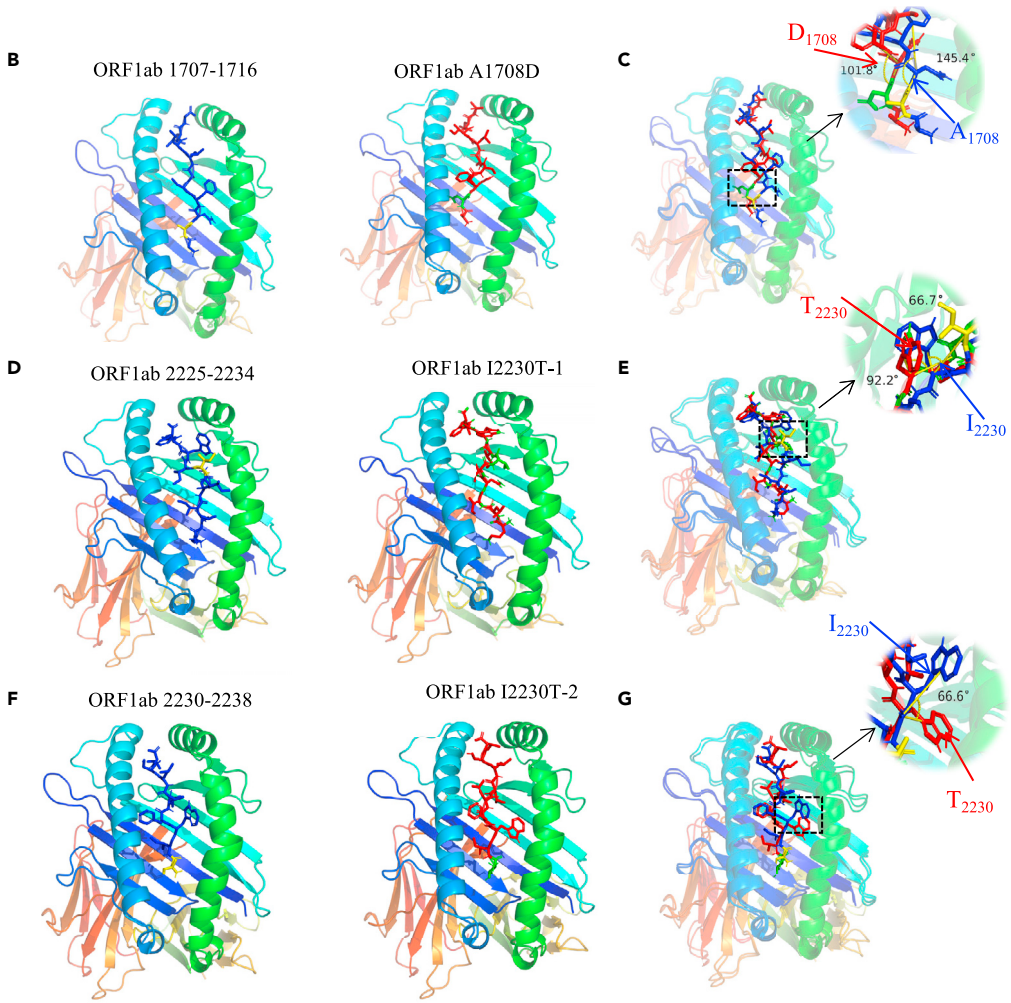

Figure 6. Computational molecular docking simulation of ancestral and mutant antigenic peptides with HLA-A2 molecule

Galaxypepdock was used for molecular docking simulation to demonstrate the structural interaction of HLA-A2 and peptides from ancestral or mutant.

(A) Summary of molecule docking simulation.

(B and C) Structures of ORF1ab 1707-1716 (B, blue stick) and ORF1ab A1708D (B, red stick) were compared in B (angle from 145.4° to 101.8°).

(D and E) Structures of ORF1ab 2225-2234 (D, blue stick) and ORF1ab I2230T (D, red stick) were compared in (D) (angle from 66.7° to 92.2°).

(F and G) Structures of ORF1ab 2230-2238 (F, blue stick) and ORF1ab I2230T (F, red stick) were compared in (F) (angle from 0 to 66.6°).

SUPPLEMENTAL INFORMATION

Supplemental information can be found online at https://doi.org/10.1016/j.isci.2022.103934.

ACKNOWLEDGMENTS

This work was supported by grants from the National Key Research and Development Program of China (2018YFC2002003), the Natural Science Foundation of China (U1801285, 81971301, and 92169102), Guangzhou Planned Project of Science and Technology (201904010111, 202002020039), Zhuhai Planned Project of Science and Technology (ZH22036302200067PWC), and the Initial Supporting Foundation of Jinan University.

AUTHOR CONTRIBUTIONS

G.C., P.W., and L.X. designed the project. C.X. performed the experiments. L.M. performed the molecular docking simulation. L.X., Z.W., G.Z., and Z.Y. analyzed the clinical information and performed the sample collection. L.G. and J.S. assisted with experiments. X.C., L.M., J.Y., Y.H., J.X., W.J. H.N., and F.G. assisted with clinical information and sample collection. C.Q., O.J.L., P.W., and G.C. analyzed the data. O.J.L. assisted with data analysis. C.X., G.C., and P.W. wrote the manuscript.

DECLARATION OF INTERESTS

The authors declare no competing interests.

Received: April 28, 2021
Revised: September 29, 2021
Accepted: February 14, 2022
Published: March 18, 2022

REFERENCES

Bertoglio, F., Meier, D., Langreder, N., Steinke, S., Rand, U., Simonelli, L., Heine, P., Ballmann, R., Schneider, K., Roth, K., et al. (2021). SARS-CoV-2 neutralizing human recombinant antibodies selected from pre-pandemic healthy donors binding at RBD-ACE2 interface. Nat. Commun. *12*, 1577.

Braun, J., Loyal, L., Frentsch, M., Wendisch, D., and Thiel, A. (2020). SARS-CoV-2-reactive T cells in healthy donors and patients with COVID-19. Nature *587*, 270–274.

Calistri, P., Amato, L., Puglia, I., Cito, F., Di Giuseppe, A., Danzetta, M., Morelli, D., Di Domenico, M., Caporale, M., Scialabba, S., et al. (2021). Infection sustained by lineage B.1.1.7 of SARS-CoV-2 is characterised by longer persistence and higher viral RNA loads in nasopharyngeal swabs. Int. J. Infect. Dis. *105*, 753–755.

Challen, R., Brooks-Pollock, E., Read, J.M., Dyson, L., Tsaneva-Atanasova, K., and Danon, L. (2021). Risk of mortality in patients infected with SARS-CoV-2 variant of concern 202012/1: matched cohort study. BMJ *372*, n579.

Collier, D.A., De Marco, A., Ferreira, I.A.T.M., Meng, B., Datir, R., Walls, A.C., Kemp S, S.A., Bassi, J., Pinto, D., Fregni, C.S., et al. (2021). Sensitivity of SARS-CoV-2 B.1.1.7 to mRNA vaccine-elicited antibodies. Nature *593*, 136–141.

Davies, N., Abbott, S., Barnard, R., Jarvis, C., Kucharski, A., Munday, J., Pearson, C., Russell, T., Tully, D., Washburne, A., et al. (2021). Estimated transmissibility and impact of SARS-CoV-2 lineage B.1.1.7 in England. Science *372*, eabg3055.

Ferreras, C., Pascual-Miguel, B., Mestre-Durán, C., Navarro-Zapata, A., Clares-Villa, L., Martín-Cortázar, C., De Paz, R., Marcos, A., Vicario, J., Balas, A., et al. (2021). SARS-CoV-2-specific memory T lymphocytes from COVID-19 convalescent donors: identification, biobanking,

and large-scale production for adoptive cell therapy. Front. Cell Dev. Biol. *9*, 620730.

Ferretti, A.P., Kula, T., Wang, Y., Nguyen, D., Weinheimer, A., Dunlap, G.S., Xu, Q., Nabilsi, N., Perullo, C.R., and Cristofaro, A.W. (2020). Unbiased screens show CD8+ T cells of COVID-19 patients recognize shared epitopes in SARS-CoV-2 that largely reside outside the spike protein. Immunity *53*, 1095–1107.e3.

Gangaev, A., Ketelaars, S.L.C., Isaeva, O.I., Patiwael, S., Dopler, A., Hoefakker, K., De Biasi, S., Gibellini, L., Mussini, C., Guaraldi, G., et al. (2021). Identification and characterization of a SARS-CoV-2 specific CD8+ T cell response with immunodominant features. Nat. Commun. *12*, 2593.

González-Galarza, F.F., Takeshita, L.Y.C., Santos, E.J.M., Kempson, F., Maia, M.H.T., da Silva, A.L.S., Teles e Silva, A.L., Ghattaoraya, G.S., Alfirevic, A., Jones, A.R., and Middleton, D. (2015). Allele frequency net 2015 update: new features for HLA epitopes, KIR and disease and HLA adverse drug reaction associations. Nucleic Acids Res. *43*, D784–D788.

Greaney, A.J., Loes, A.N., Crawford, K.H., Starr, T.N., and Bloom, J.D. (2021). Comprehensive mapping of mutations to the SARS-CoV-2 receptor-binding domain that affect recognition by polyclonal human serum antibodies. Cell Host Microbe. https://doi.org/10.1101/2020.12.31.425021.

Grifoni, A., Weiskopf, D., Ramirez, S.I., Mateus, J., and Sette, A. (2020). Targets of T cell responses to SARS-CoV-2 coronavirus in humans with COVID-19 disease and unexposed individuals. Cell *181*, 1489–1501.e15.

Hasup, L., Lim, H., Sup, L.M., and Chaok, S. (2015). GalaxyPepDock: a protein–peptide docking tool based on interaction similarity and energy optimization. Nucleic Acids Res. *43*, 431–435.

He, Y., Li, J., Mao, W., Zhang, D., Liu, M., Shan, X., Zhang, B., Zhu, C., Shen, J., Deng, Z., et al. (2018). HLA common and well-documented alleles in China. HLA *92*, 199–205.

Jackson, L.A., Anderson, E.J., Rouphael, N.G., Roberts, P.C., and Beigel, J.H. (2020). An mRNA vaccine against SARS-COV-2 — preliminary report. N. Engl. J. Med. *383*, 1920–1931.

Kemp, S., Meng, B., Datir, R., Collier, D., Ferreira, I., Carabelli, A., Harvey, W., Robertson, D., and Gupta, R. (2020a). Recurrent emergence and transmission of a SARS-CoV-2 Spike deletion ΔH69/V70. https://www.biorxiv.org/content/10.1101/2020.12.14.422555v6.

Kemp, S.A., Collier, D.A., Datir, R., Gayed, S., and Gupta, R.K. (2020b). Neutralising antibodies drive spike mediated SARS-CoV-2 evasion. Preprint at medRxiv. https://doi.org/10.1101/2020.12.05.20241927.

Kirby, T. (2021). New variant of SARS-CoV-2 in UK causes surge of COVID-19. Lancet Respir. Med. *9*, e20–e21.

Lauring, A.S., and Hodcroft, E.B. (2021). Genetic variants of SARS-CoV-2—what do they mean? JAMA *325*, 529–531.

Le Bert, N., Tan, A.T., Kunasegaran, K., Tham, C.Y.L., Hafezi, M., Chia, A., Chng, M.H.Y., Lin, M., Tan, N., Linster, M., et al. (2020). SARS-CoV-2-specific T cell immunity in cases of COVID-19 and SARS, and uninfected controls. Nature *584*, 457–462.

Mani, S., S, D., Ragunathan, V., Tiwari, P., Arumugam, S., and Parthiban, B. (2020). Molecular docking, validation, dynamics simulations, and pharmacokinetic prediction of natural compounds against the SARS-CoV-2 main-protease. J. Biomol. Struct. Dyn. *38*, 1–28.

Muik, A., Wallisch, A., Sänger, B., Swanson, K., Mühl, J., Chen, W., Cai, H., Maurus, D., Sarkar, R., Türeci, Ö., et al. (2021). Neutralization of SARS-CoV-2 lineage B.1.1.7 pseudovirus by BNT162b2 vaccine-elicited human sera. Science *371*, 1152–1153.

Neches, R., Kyrpides, N., and Ouzounis, C. (2021). Atypical divergence of SARS-CoV-2 Orf8 from Orf7a within the coronavirus lineage suggests potential stealthy viral strategies in immune evasion. mBio *12*, e03014–e03020.

Parker, M.D., Lindsey, B.B., Shah, D.R., Hsu, S., Keeley, A.J., Partridge, D.G., Leary, S., Cope, A., State, A., Johnson, K., et al. (2021). Altered subgenomic RNA expression in SARS-CoV-2 B.1.1.7 infections. Preprint at bioRxiv. https://doi.org/10.1101/2021.03.02.433156.

Peacock, T.P., Goldhill, D.H., Zhou, J., Baillon, L., and Barclay, W.S. (2020). The furin cleavage site of SARS-CoV-2 spike protein is a key determinant for transmission due to enhanced replication in airway cells. Preprint at bioRxiv. https://doi.org/10.1101/2020.09.30.318311.

Polack, F.P., Thomas, S.J., Kitchin, N., Absalon, J., Gurtman, A., Lockhart, S., Perez, J.L., Pérez Marc, G., Moreira, E.D., Zerbini, C., et al. (2020). Safety and efficacy of the BNT162b2 mRNA covid-19 vaccine. N. Engl. J. Med. *383*, 2603–2615.

Qiu, C., Wang, Z., Xiao, C., Chen, X., and Chen, G. (2020). CD8+ T cell epitope variations suggest a potential antigen presentation deficiency for spike protein of SARS-CoV-2. SSRN Electron. J. https://doi.org/10.2139/ssrn.3720772.

Rashid, F., Dzakah, E., Wang, H., and Tang, S. (2021). The ORF8 protein of SARS-CoV-2 induced endoplasmic reticulum stress and mediated immune evasion by antagonizing production of interferon beta. Virus Res. *296*, 198350.

Sahin, U., Muik, A., Vogler, I., Derhovanessian, E., Kranz, L.M., Vormehr, M., Quandt, J., Bidmon, N., Ulges, A., Baum, A., et al. (2020). BNT162b2 induces SARS-CoV-2-neutralising antibodies and T cells in humans. Preprint at medRxiv, 2020.2012.2009.20245175.

Seow, J., Graham, C., Merrick, B., Acors, S., Pickering, S., Steel, K., Hemmings, O., O'Byrne, A., Kouphou, N., Galao, R., et al. (2020). Longitudinal observation and decline of neutralizing antibody responses in the three months following SARS-CoV-2 infection in humans. Nat. Microbiol. *5*, 1598–1607.

Starr, T., Greaney, A., Hilton, S., Crawford, K., Navarro, M., Bowen, J., Tortorici, M.A., Walls, A., Veesler, D., and Bloom, J. (2020). Deep mutational scanning of SARS-CoV-2 receptor binding domain reveals constraints on folding and ACE2 binding. Cell *182*, 1295–1310.e20.

Tarke, A., Sidney, J., Kidd, C.K., Dan, J.M., and Sette, A. (2021a). Comprehensive analysis of T cell immunodominance and immunoprevalence of SARS-CoV-2 epitopes in COVID-19 cases. Cell Rep. Med. *2*, 100204.

Tarke, A., Sidney, J., Methot, N., Zhang, Y., and Sette, A. (2021b). Negligible impact of SARS-CoV-2 variants on CD4 + and CD8 + T cell reactivity in COVID-19 exposed donors and vaccinees. Preprint at bioRxiv. https://doi.org/10.1101/2021.02.27.433180.

Volz, E., Mishra, S., Chand, M., Barrett, J.C., and Ferguson, N.M. (2021). Transmission of SARS-CoV-2 Lineage B.1.1.7 in England: insights from linking epidemiological and genetic data. Preprint at medRxiv. https://doi.org/10.1101/2020.12.30.20249034.

Wang, P., Nair, M.S., Liu, L., Iketani, S., Luo, Y., Guo, Y., Wang, M., Yu, J., Zhang, B., Kwong, P.D., et al. (2021). Antibody resistance of SARS-CoV-2 variants B.1.351 and B.1.1.7. Nature *593*, 130–135.

Ward, H., Cooke, G., Atchison, C., Whitaker, M., and Elliott, P. (2020). Declining prevalence of antibody positivity to SARS-CoV-2: a community study of 365,000 adults. Preprint at medRxiv. https://doi.org/10.1101/2020.10.26.20219725.

Weiskopf, D., Schmitz, K.S., Raadsen, M.P., Grifoni, A., and Vries, R.D.D. (2020). Phenotype and kinetics of SARS-CoV-2-specific T cells in COVID-19 patients with acute respiratory distress syndrome. Sci. Immunol. *5*, eabd2071.

Wheatley, A., Juno, J., Wang, J., Selva, K., Reynaldi, A., Tan, H., Lee, W., Wragg, K., Kelly, H., Esterbauer, R., et al. (2021). Evolution of immune responses to SARS-CoV-2 in mild-moderate COVID-19. Nat. Commun. *12*, 1162.

Wu, A., Peng, Y., Huang, B., Ding, X., and Jiang, T. (2020). Genome composition and divergence of the novel coronavirus (2019-nCoV) originating in China. Cell Host Microbe *27*, 325–328.

Xiao, C., Qiu, C., Deng, J., Ye, J., Gao, L., Su, J., Luo, O.J., Wang, P., and Chen, G. (2021). Optimization of antigen-specific CD8+ T cell activation conditions for infectious diseases including COVID-19. STAR Protoc. *2*, 100789.

Yurkovetskiy, L., Wang, X., Pascal, K.E., Tomkins-Tinch, C., Nyalile, T., Wang, Y., Baum, A., Diehl, W.E., Dauphin, A., and Carbone, C. (2020). Structural and Functional Analysis of the D614G SARS-CoV-2 Spike Protein Variant (Social Science Electronic Publishing).

Zahradnik, J., Marciano, S., Shemesh, M., Zoler, E., and Schreiber, G. (2021). SARS-CoV-2 RBD in vitro evolution follows contagious mutation spread, yet generates an able infection inhibitor. Preprint at bioRxiv. https://doi.org/10.1101/2021.01.06.425392.

Zhang, F., Gan, R., Zhen, Z., Hu, X., Li, X., Zhou, F., Liu, Y., Chen, C., Xie, S., Zhang, B., et al. (2020). Adaptive immune responses to SARS-CoV-2 infection in severe versus mild individuals. Signal. Transduct. Target. Ther. *5*, 156.

STAR★METHODS

KEY RESOURCES TABLE

REAGENT or RESOURCE	SOURCE	IDENTIFIER
Antibodies		
PE anti-human HLA A2 (clone BB7.2)	BioLegend	Cat#343305;RRID:AB_1877228
FITC anti-human HLA-A2 (clone BB7.2)	BioLegend	Cat#343303;RRID:AB_1659246
PerCP labelled human $CD8^+$ (clone SK1)	BioLegend	Cat#344708;RRID:AB_1967149
APC labelled human $CD8^+$ (clone T8)	BioLegend	Cat#301049;RRID:AB_2562054
APC labelled human CCR7 (clone G043H7)	BioLegend	Cat#353212;RRID:AB_10916390
FITC labelled human CD45RA (clone HI100)	BioLegend	Cat#304150; RRID:AB_2564158
anti-human CD28 Antibody (clone CD28.2)	BioLegend	Cat#302901; RRID:AB_314303
APC anti-human CD69 (clone FN50)	BioLegend	Cat#310909;RRID:AB_314844
APC Annexin V	BioLegend	Cat#640919
PerCP anti-human IFN-γ (clone 4S.B3)	BioLegend	Cat#502524;RRID:AB_2616613
FITC anti-human Granzyme B (clone GB11)	BioLegend	Cat#515403;RRID:AB_2114575
Biological samples		
Blood samples from healthy donors, COVID-19 convalescent	Guangzhou Blood Center, Guangzhou Center for Disease Control and Prevention	N/A
Chemicals, peptides, and recombinant proteins		
Lymphocyte separation medium	GE	Cat#MQ0148
Fetal bovine serum	LONSERA	Cat#S711-001S
Dimethyl sulfoxide	Sigma-Aldrich	Cat#D2650
MHC monomer	BioLegend	Cat#280003
PE streptavidin	BioLegend	Cat#405203
Mitomycin C	sinochem	Cat#50-07-7
CFSE	TargetMol	Cat#T6802
IL-2	SL PHARM	N/A
GolgiPlug	BD Biosciences	Cat#550583
50 mM biotin	Invitrogen	Cat#2110450
Critical commercial assays		
pMHC ELISA Kit	Mlbio	Cat#1269746
EasySep Human negative selection CD8 T	Stemcell	Cat#17953
Experimental models: Cell lines		
T2-A2	Dr. Anna Gil	N/A
Software and algorithms		
FlowJo software version 10.7	FlowJo LLC	https://www.flowjo.com/
Prism version 8	Graphpad	https://www.graphpad.com/
SPSS Statistics 22	IBM	https://www.ibm.com/
Other		
Each epitope corresponds to a tetramer	Home-made	N/A

RESOURCE AVAILABILITY

Lead contact

Further information and requests for resources and reagents should be directed to and will be fulfilled by the Lead contact, Guobing Chen (guobingchen@jnu.edu.cn).

Materials availability

The corresponding tetramers may be obtained from the research group of Guobing Chen, Jinan University, China.

Data and code availability

All data reported in this paper will be shared by the lead contact upon request.

This paper does not report original code.

Any additional information required to reanalyze the data reported in this paper is available from the lead contacts upon request.

EXPERIMENTAL MODEL AND SUBJECT DETAILS

Human subjects

The Institutional Review Board of the School of Medicine of Jinan University approved this study (JNUKY-2021-009). Unexposed donors were healthy individuals enrolled in Guangzhou Blood Center and confirmed with a negative report for SARS-CoV-2 RNA real-time reverse transcriptase polymerase chain reaction (RT-PCR) assay. These donors had no known history of any significant systemic diseases, including, but not limited to, hepatitis B or C, HIV, diabetes, kidney or liver diseases, malignant tumors, or autoimmune diseases. Convalescent donors included subjects who were hospitalized for COVID-19 or confirmed SARS-CoV-2 infection by RT-PCR assay. SARS-CoV-2 vaccinees were also recruited 1-3 months after vaccination with the inactivated vaccine (Beijing Institute of Biological Products of Sinopharm). All subjects provided informed consent at the time of enrollment that their samples could be used for this study. Complete blood samples were collected in acid citrate dextrose tubes and stored at room temperature prior to peripheral blood mononuclear cells (PBMCs) isolation and plasma collection. PBMCs were isolated by density gradient centrifugation using lymphocyte separation medium (GE). Starting with a single cell suspension of human PBMCs, the $CD8^+$ T cell content of the isolated fraction is typically 95%. After isolation, the cells were cryopreserved in fetal bovine serum (LONSERA) with 10% dimethyl sulfoxide (DMSO) (Sigma-Aldrich) until use.

METHOD DETAILS

HLA-A2 restricted T cell epitope prediction

The spike (S), membrane (M), nucleocapsid (N) and ORF protein sequences of SARS-CoV-2 Wuhan-Hu-1 strain (NC_045512.2) were used for T cell epitope prediction with the "MHC I Binding"tool (http://tools.iedb.org/mhci). The prediction method used was IEDB Recommended 2.22 (NetMHCpan EL), with MHC allele selected as HLA-A*02:01, the most frequent class I HLA genotype among Chinese population (González-Galarza et al., 2015; He et al., 2018). All predicted epitopes containing the same amino acid residue corresponding to the mutation from B.1.1.7 were compared. The peptide with the best prediction score was used as the candidate epitope for ancestral Wuhan strain. Meanwhile, peptides with identical amino acid sequences except for the mutated point were used as candidate epitopes for variant B.1.1.7.

Peptide screening in T2A2 cells

The candidate peptides were synthesized in GenScript Biotechnology Co., Ltd (Nanjing, China) and resuspended in DMSO at a concentration of 10 mM, respectively. T2A2 cells were seeded into 96-well plates, and then incubated with peptides at a final concentration of 20 μM at 37°C for 4 hours. Set DMSO as blank control, Influenza A M1 peptide (GILGFVFTL) as positive control, and Zika virus peptide (GLQRLGYVL) as negative control. Cells were stained with PE anti-human HLA-A2 antibody (BioLegend) at 4°C in the dark for 30 min, and acquired in flow cytometer FACS Canto (BD).

Enzyme-linked immunosorbent assay

10 mM peptide stock solution was diluted to 400 μM in PBS. 20 μL diluted peptide and 20 μL 1 μg/mL UV-sensitive peptide HLA-A2 monomer (BioLegend) were added into 96-well plates and mixed well by pipetting up and down. The plates were then exposed to UV light (365 nm) for 30 min on ice, and incubated for 30 min at 37°C in the dark. Finally, 40 μL of peptide-exchanged monomer was used for test. The pMHC level was determined by using a pMHC ELISA Kit (Mlbio). Within 15 min after adding stop solution, the

absorbance values of sample were read at 450 nm. Set UV-irradiated monomers as blank control, Influenza A M1 peptide (GILGFVFTL) as positive control, and Zika virus peptide (GLQRLGYVL) as negative control.

Generation of antigen specific HLA-A2 tetramer

30 μL peptide-exchanged monomer formed in the above steps was mixed with 3.3 μL PE streptavidin (Bio-Legend) on a new plate and incubated on ice in the dark for 30 min. 2.4 μL blocking solution (1.6 μL 50 mM biotin plus 198.4 μL PBS) was added to stop the reaction and incubated at 4-8°C overnight.

Cell-surface CD8, CCR7, CD45RA and tetramer staining

PBMCs were isolated from peripheral venous blood of healthy donors, convalescent COVID-19 patients and SARS-CoV-2 vaccinees. The HLA-$A2^+$ donors were identified by using flow cytometry. Briefly, 10^6 PBMCs were stained with FITC anti-human HLA-A2 antibody (BioLegend) at 4°C in the dark for 30 min, and acquired by using flow cytometer. HLA-A2 positive PBMCs samples were further stained with PE labeled tetramer (home-made), PerCP labeled human $CD8^+$ antibody (BioLegend), APC labeled human CCR7 antibody (BioLegend), FITC labeled human CD45RA antibody (BioLegend) and acquired with flow cytometer FACS Canto (BD).

Activation and cytotoxicity analysis of $CD8^+$ T cells

HLA-A2 expressing T2A2 cells were loaded with peptides for subsequent T cell activation. Briefly, T2A2 cells were treated with 20 μg/mL mitomycin C (Sinochem) for 30 min to stop cell proliferation, and loaded with given epitope peptides. 0.5×10^6 $CD8^+$ T cells isolated from health donors were co-cultured with 0.5×10^6 peptide-loaded T2A2 cells stained with 5 μmol/L CFSE (TargetMol), and stimulated with 1 μg/mL anti-human CD28 antibodies (BioLegend) and 50 IU/mL IL-2 (SL PHARM, Recombinant Human Interleukin-2(^{125}Ala) Injection). 50 IU/mL IL-2 and 20 μM mixed peptides were then supplemented every two days. The T cell activation marker CD69 (BioLegend), tetramer specific $CD8^+$ T cells and apoptosis marker Annexin V-APC (BioLegend) on T2A2 cells were evaluated after 16 hours and 7 days, respectively. On day 7, stimulatory T cell-mediated T2A2 killing, we gated the total $CD8^+$ (CFSE negative) and T2A2 cells (CFSE positive), then stained with LIVE/DEAD dye and then calculated the percentage of live T2A2 cells. On day 7, cells were re-stimulated with peptides for 6 hours in the presence of Leuko Act Cktl with GolgiPlug (BD) plus 50 IU/mL IL-2, and the production of IFN-γ and Granzyme B was checked with PerCP anti-human IFN-γ (BioLegend) and FITC anti-human Granzyme B (BioLegend) staining.

Molecular docking simulation of peptide-HLA-A2 complex

To evaluate the binding pattern and affinity of peptides with HLA-A2, molecular docking simulation was carried out with Galaxypepdock. The available structure of HLA: 0201 (PDB ID: 3mrb) was downloaded from the RSCB PDB server (https://www.rcsb.org/) for modeling. Galaxypepdock is a template-based docking program for peptides and proteins, which can generate 10 models to evaluate the results of the docking (Hasup et al., 2015; Mani et al., 2020). The top model with the highest interaction similarity score was selected and visualized by using Discovery Studio 4.5. PyMol 1.1 software was used to calculate the angle deflection of benzene ring in the polypeptide, and used the central atoms of three amino acids to calculate the angle.

Statistical analysis

The data were analyzed by one-way ANOVA and paired-samples t-tests for statistical significance by using Graphpad prism 8 and SPSS 22.0 software. *P* value less than 0.05 was considered to be statistically significant.